ARMY RESEARCH LABORATORY

Surface Heating of Molybdenum, Tantalum, and Tungsten Rods by Pulsed Currents

Charles R. Hummer
John D. Powell
Paul R. Berning

ARL-TR-2843 **NOVEMBER 2002**

NOTICES

Disclaimers

The findings in this report are not to be construed as an official Department of the Army position unless so designated by other authorized documents.

Citation of manufacturers' or trade names does not constitute an official endorsement or approval of the use thereof.

DESTRUCTION NOTICE—Destroy this report when it is no longer needed. Do not return it to the originator.

Army Research Laboratory
Aberdeen Proving Ground, MD 21005-5066

ARL-TR-2843 November 2002

Surface Heating of Molybdenum, Tantalum, and Tungsten Rods by Pulsed Currents

Charles R. Hummer, John D. Powell, and Paul R. Berning
Weapons and Materials Research Directorate

ACKNOWLEDGMENTS

The authors would particularly like to thank Mr. Mike Keele of the U.S. Army Research Laboratory (ARL) for designing the electrode assembly and for participating in a series of initial experiments of a similar nature. These efforts were very important in the planning and execution of the measurements reported herein. Mr. Alex Zielinski of ARL is thanked for valuable discussions and a thorough review of this report. The experimental assistance of Dr. Clinton Hollandsworth of Dynamic Sciences, Incorporated, and the support and encouragement of Dr. Andrus Niiler and Dr. William Bruchey of ARL are gratefully acknowledged.

Mr. Keith Mahan of ARL prepared most of the samples and provided invaluable technical support throughout the course of these experiments.

Contents

Figures

Tables

SURFACE HEATING OF MOLYBDENUM, TANTALUM, AND TUNGSTEN RODS BY PULSED CURRENTS

1. Introduction

A large and active international community of researchers is devoted to the establishment of accurate thermophysical parameters for most elements and their alloys. This community publishes recommended values for quantities such as specific heat, thermal conductivity, and resistivity for these materials. For decades, pulsed heating experiments have played a crucial role in the determination of these parameters **[1,2]**. Such experiments have certain advantages over steady state or quasi-steady state experiments for many measurements, particularly for temperatures above 2000 K. These advantages include the reduction or elimination of corrections for radiation losses from the sample, and the elimination of complications attributable to chemical reactions, evaporation, or loss of mechanical strength. Indeed, for temperatures near and above the melting point of the material, pulsed experiments are essential in order to prevent hydrodynamic collapse of unconfined samples during the measurement cycle.

Generally, the pulsed heating experiments just described are conducted in either the millisecond or microsecond time domain. Two types of samples are used in these experiments. In the millisecond time domain, sometimes referred to as the sub-second time domain, the sample is usually a hollow tube a few millimeters in diameter and about 1 mm thick, whereas the samples for the microsecond experiments tend to be thin wires or foils, usually much less than a millimeter in thickness. In many cases, the time-dependent diffusion of magnetic fields and currents into the sample can be ignored or treated by analytical approximations. A recent experiment by Kaschnitz and Reiter **[3]** illustrates the different procedures associated with measurement in both time domains.

Simple estimates of the time to achieve local thermal equilibrium in a metal (based on conductivity considerations) suggest that even for heating times in the sub-microsecond region, equilibrium conditions should prevail. Measurements of thermophysical parameters, such as those discussed previously, are done usually with samples thin enough that "global equilibrium" and a uniform temperature within the sample are quickly attained. This condition permits a determination of enthalpy and enthalpy changes within the sample, which is key to the measurement of specific heat and resistivity. However, there appears to be some question as to whether rate effects might exist on or near the surface at current densities and heating rates comparable to those realized in the present experiment, 3×10^{10} A/m^2 and 10^8 K/s, respectively.

Many military applications of pulsed power and electromagnetic technology involve currents on the order of 100 kA or greater and heating times in the microsecond range. In these applications, the conductors are too large to ignore skin depth effects and heat transport within the sample. A

complete description of effects related to size is required. For this reason, an exploratory effort to study the behavior of particular metals and alloys that are heated electrically to high temperatures in times on the order of 100 μs to 200 μs is under way at the U.S. Army Research Laboratory (ARL). In these experiments, a capacitor bank supplies large electrical currents that reverse direction about every 75 μs. The purpose of this work is threefold. First, there is a requirement to provide data to validate numerical computer codes developed to support Army applications of pulsed power. Second, data are not available for some materials of special interest to the Army, and it is desired to provide these data. Finally, it is desirable to provide additional data to clarify the situation with regard to possible heating rate effects.

In the present experiments, the pulsed current, sample geometry, specific heat, and resistivity largely determine the distribution of temperature throughout the sample and the voltage produced across the sample. Thus, measurement of the voltage across a portion of the sample and the current through it provides information about the validity of these parameters. Theoretical calculations that couple the diffusion of current with heat transport in the sample **[4]** are then required in order to properly interpret the measured voltage.

Because of the sample size and the time profile of the pulsed current in our experiments, equilibrium conditions for temperature and energy distribution throughout the sample are never realized, in contrast to the experiments discussed previously. The voltage we measure is a "surface voltage"; the voltage drop along the center of the rod or any other line element generally will be different from our measured voltage. Furthermore, because of the large currents and the relatively rapid current reversals, the measured voltage has a resistive component (the quantity of interest) and a non-negligible inductive component. The two can be separated for a fixed measurement loop if the loop inductance is known.

If the determination of the surface resistive voltage (the principal focus of the experimental measurements) is accurate, the surface temperature should then be the value predicted by the calculation. However, to have complete confidence in the validity of our rather indirect procedure, it is desirable to perform at least some limited temperature measurements. We have used a particularly simple and direct technique, based on the detection of infrared radiation with a charge-coupled device (CCD) TV camera, to measure the surface temperature of all three materials at temperatures near 800 K.

The principal purpose of this report is to provide experimental data that can be compared with the results of theoretical calculations. Through this approach, we can validate our computer codes and assess the accuracy of our experimental techniques. For a first study, it is obviously desirable to employ materials whose thermophysical properties are very accurately known. Such is the case for the refractory elements molybdenum, tantalum, and tungsten. The specific heat and resistivity for these elements are available as an evaluated data set accurate to about 3%, except near the melting temperatures. Accordingly, this report is concerned primarily with these three materials.

The general outline of this report is as follows. In Section 2, we discuss the experimental arrangement, including the sample holder, the voltage probes, and the electrical power source and diagnostics. This section also includes a discussion of the procedures used in the voltage measurements and the temperature measurements (these measurements are not done simultaneously). Section 3 provides a description of the theoretical calculations and the flux-loop geometry used in the experiment. Section 4 provides the results of the calculations and the experiments. Both sets of results are carefully compared. Section 5 presents the discussion of an iterative procedure that couples theory and experiment to determine the resistivity as a function of temperature for substances for which this property is not known. Finally, our conclusions and recommendations for future work are given in Section 6.

2. Experimental Setup and Procedures

2.1 Electrical Power Source and Diagnostics

The heating source is a 1600 μF capacitor bank consisting of eight 200 μF capacitors. A 40 mΩ resistor, attached directly to the terminal of each capacitor, limits the output current. Two RG-217 coaxial cables carry the current from each capacitor to the input terminals of a triggered vacuum switch **[5]**. The output of the switch is coupled through 16 coaxial cables to two electrode plates, as shown in Figure 1. The electrodes were fabricated from an aluminum alloy. The mean distance from the outer coaxial cable conductors to the center of the sample was 330 mm; sample diameters varied from 3.96 mm to 6.35 mm. The electrode spacing was maintained at 76 mm.

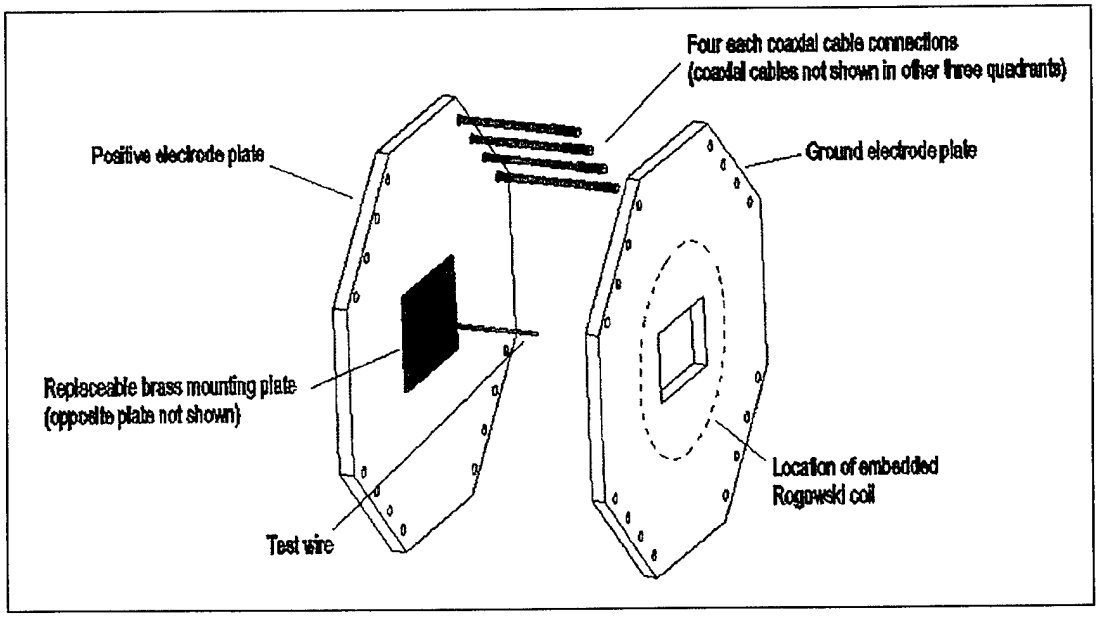

Figure 1. Experimental arrangement.

The outer copper braids of the coaxial cables are attached to brass fittings threaded into the ground plate of the test stand. The copper center conductor, surrounded by a polyethylene core, is carried through the gap to the second plate where the conductor makes electrical contact with the second or "hot" plate. The electrodes and capacitors are housed in a limited access range, whereas the charging unit and some recording instruments are in a remote control room. The vacuum switch is triggered remotely after the capacitor bank is charged to the desired voltage.

Current and voltage measurements are required in order to compare theory and experiment. To avoid errors associated with the differentiation or integration of recorded signals, the current and the derivative of the current (I-dot) are measured separately. Four wide-band current transformers (i.e., Pearson coils[1]) are used to measure the total current from the capacitor bank. The center conductors of the cables attached to each of two capacitors are routed through the center of a Pearson coil. The connections become coaxial again at the periphery of the capacitor container. A Rogowski belt embedded in the ground plate of the electrode assembly (see Figure 1) measures the derivative of the current. The current transformer signals were recorded in transient digitizers in the control room. The high impedance of the voltage probes and the desired high frequency response require connecting cable lengths to be small. Therefore, the voltage signals and the I-dot signal were recorded with a digital oscilloscope near the electrodes in the range area. The existence of two different time bases in the recording instruments resulted in a small contribution to the uncertainty in the accuracy of our measurements.

2.2 Voltage Measurement Procedure

Although the rise time in our experiment, approximately 20 μs, is not particularly fast, the large peak currents, from 200 to 400 kA, produce large inductive voltages in the pulsed power circuit. These large voltages impose two requirements on the measurement circuit. The first is the necessity to perform differential measurements in order to eliminate any voltage drop in the electrode grounding circuit. Two high voltage probes referenced to the ground plate of the electrode assembly are used for this purpose. The resistance of each is 1000 MΩ; this high resistance ensures that the measurement current does not contribute to the flux voltage in the loop (the typical voltage across the sample is <2 kV). Equally important, the high impedance also reduces errors attributable to contact resistance effects. The frequency response and the attenuation of both probes were determined with a square-wave pulse generator before each measurement. If necessary, the frequency compensation circuits of the probes were readjusted to ensure that the measurements were sufficiently accurate.

The second requirement is to perform measurements with a well-defined loop so that corrections can be made for the induced voltage generated by the changing magnetic flux. A straightforward determination of the inductance can be made if the loop is fixed, does not enclose current-carrying conductors, and is in a region of high symmetry where the induction field is readily calculated. A loop that is not too close to the electrodes and that extends from the surface of the

[1]Pearson Electronics, Inc., Model 1423

sample (see Figure 1) to a distance several millimeters from the surface approximates that condition for our experimental arrangement. The flux, Φ, linking the rod and the measurement circuit is given by

$$\Phi = M I \tag{1}$$

in which M is the mutual inductance and I is the current. The mutual inductance can be calculated from Ampere's law and the inductive voltage can then be determined by multiplication of the time-dependent derivative of the sample current by the constant M, i.e.,

$$Vr_E = V_M - M\, dI/dt, \tag{2}$$

in which Vr_E is the deduced resistive voltage drop, and V_M is the experimentally measured voltage.

Additional factors influence the design of the flux loop and attachment of the voltage probes to the sample. Because we measure a surface voltage, it is important to have contact along a considerable angular region of the sample in order to average irregularities in the sample surface. A variety of sized spring clips, either Be-Cu or stainless steel, were used to provide direct contact with the sample. They are of such a design that one might expect contact between 180 and 270 degrees of the cylindrical surface of the sample.

The preceding discussion of the inductive component of the voltage considered only the voltage produced by the time-dependent magnetic induction field that results from a changing current. If the current source or the flux loop moves, an additional contribution to the inductive voltage is produced. To prevent a contribution from this source, it was necessary to provide some inertia for the flux loop itself. This objective was achieved with blocks of G-10 material, an E-glass and epoxy composite, to provide a form for the measurement loop. The straight section of each clip was inserted into a drilled hole in the G-10 block. Leads from the remotely located voltage probes were twisted to eliminate flux loops between the leads and then threaded into the block and attached to the spring clips. Flux loops of different size and shapes were used throughout the experiment; they are described in the theory discussion in Section 3. To prevent interference with the voltage measurements by plasma currents from the region of contact between the sample and the electrodes, plasma shields were installed on the inner faces of the electrodes. The shields were 3 mm thick rectangles made of G-10 with a center hole to accommodate the sample diameter.

The theory for the heating of the rod and the interpretation of the experimental data are based on the assumption that the current distribution in the plates and the rod is axially symmetrical. To avoid disassembling the system each time a sample is changed, it is necessary to provide access to the central region by leaving gaps in the cable arrays—something accomplished by the octagonal plate design of Figure 1. These gaps destroy the complete symmetry of the configuration; nevertheless, this arrangement results in a nearly axisymmetrical current distribution at the sample.

Because the electrical connections are far from the sample, the current distribution becomes axially symmetrical near the rod. This symmetry was demonstrated by a simple two-dimensional calculation in which the electrical contacts were modeled by 16 current sources, whereas a single current sink simulated the rod. This simple model showed that the magnitude of the current density was constant to within 3×10^{-3}% on a circle with a radius that is 10 times the radius of a typical rod, 3 mm. In addition, the angle between the current density direction at a point on the circle and the radial line between the point and the center of the rod was less than 1.8×10^{-3} degrees. This result indicates that the current density distribution has become nearly axially symmetrical at this radial distance. This trend toward axial symmetry continues as the radius of the circle decreases to the radius of the sample.

2.3 Temperature Measurement Technique

Because the current pulse in our experiment has the functional form of a damped sine wave that persists for about 200 μs, a continuous measurement of the temperature during this period would require specialized instrumentation. However, a thermography technique that uses standard video cameras that are sensitive to visible and infrared radiation can be used to measure the final surface temperature of a heated rod, provided that appropriate precautions and sample preparation are made. We have used such a technique in this work and have described it in detail in a previous ARL report **[6]**; only a brief description of the method is given here.

In this technique, a thermal emission image of the source is acquired, and the video levels are compared with those obtained previously by a calibration procedure. In this procedure, rods heated to various temperatures in an oven were observed by the camera and used to construct a curve of video signal level versus temperature. Our version of the technique relies on the response of an electronically shuttered camera that is sensitive to visible and near IR radiation. With this system, measurements are made over a broad spectral band extending to wavelengths below the shortest wavelength emitted by the heated sample.

The Planck distribution law for blackbody emission distribution can be used to show that for wavelengths much shorter than the value at which peak spectral radiance occurs, there is an extremely strong dependence of spectral radiance on temperature. Any system that responds across this short wavelength band (as our system does) will therefore exhibit extremely strong temperature dependence. This sensitivity to temperature change can increase the accuracy of temperature measurements, but it also limits the temperature range observed with a given setup of the camera. For example, with the lens aperture and exposure time used in the present measurements, the range of observable temperatures was only from about 700 K to 820 K.

2.3.1 The Camera

Our technique uses a video camera, the Flashcam[2], which detects the radiation in an array of CCDs. The Flashcam is a programmable, fast shutter, multiple exposure camera that responds to

[2]The Cooke Corporation, Flashcam Serial No. 335NG0041

radiant flux in the wavelength range from 350 nanometers (nm) to 1040 nm. It has an adjustable number of exposures per frame, adjustable delay times between exposures, and adjustable delay times between an external trigger and the initiation of an exposure sequence. The camera can be operated in one of two output modes, capturing a single digital image or recording images continuously in a free-run mode. The single digital image may be composed of anywhere from one to ten individual exposures. When operated in a free-run mode (no trigger), the camera resembles a normal video camera except that the video signal is obtained by re-conversion from the digital signal. In this mode, the reconverted signal is usually stored continuously on videotape.

2.3.2 Sample Preparation and Emissivity Considerations

Our procedure for the measurement of temperature involves direct comparison of video signal levels obtained in calibration runs with those observed when a pulse-heated specimen is viewed. In general, metal surfaces oxidize when heated in air, and the oxidization rates accelerate rapidly for many materials as the temperature rises above 600 K. Because the current pulse in our experiments is so brief, most of the oxidization will occur after the pulse ends, i.e., as the sample cools over a period of many seconds. It is essential in a direct comparison procedure such as ours that the sample emissivity be the same in calibration runs and the actual temperature measurements, i.e., that the samples have stable thermal emission characteristics. To minimize changes in the surface during the experiment and also during repeated heating for calibration, it is necessary to work with samples that have been oxidized previously in a controlled manner.

Dense metal oxide layers that prevent additional oxygen atoms from reaching the underlying metal atoms can be formed on the surface of molybdenum and tungsten samples at certain temperatures when the specimen is pre-heated. Our procedure was to heat each sample in an oven for 10 minutes at a temperature of about 770 K. Once prepared in this manner, molybdenum and tungsten samples tended to give very reproducible results. The more complex nature of the oxidization process in tantalum precluded the use of the same treatment for this element. Instead, a coating of high emissivity paint was used to achieve a specimen surface with reasonably stable emission characteristics. The goal of heating all samples to a final temperature of ~800 K represents a conservative choice; our method cannot be used for temperatures of 1000 K or greater because of the mechanics of the oxidization processes.

All samples were at least 99.9% pure and in the form of cylindrical rods 150 mm long. The diameter of the molybdenum and tantalum samples was 5 mm, whereas the diameter of the tungsten samples was 4 mm. The samples were used as obtained from the supplier[3].

2.3.3 Calibration Procedure

The calibration procedure was as follows. The sample was pre-heated to a selected temperature in the 700 K to 820 K range. It was then quickly removed and placed in a V-block arrangement

[3] Alfa Aesar, 30 Bond Street, Ward Hill MA 01835-8099

near the oven where it could be viewed continuously by the Flashcam camera. A blackbody simulator (BBS) was situated directly behind the V-block so that the camera viewed the sample and the simulator simultaneously. The purpose of the BBS was to aid in the selection of the appropriate lens apertures and exposure times and to act as a monitor; it was not part of the calibration procedure. The sample temperature in the oven was determined by a thermocouple. The calibration temperature was defined as the oven temperature corrected for the cooling that occurred as the sample was removed from the oven and positioned for viewing.

In successive calibration runs, video levels were recorded in both the triggered and the free-run modes of camera operation. In this manner, specific video levels could be assigned to particular temperatures for either mode of operation. When operated in the free-run mode, the video signal permitted determination of the cooling rate, observed to be approximately 10 K/s in the calibration runs and later in the pulsed heating experiments. The mechanics of removing the sample from the oven and placing it in the V-blocks for observation is the major contributor to the estimated uncertainty in our temperature measurements, ±20 K.

3. Theoretical Analysis

Calculations of the electromagnetic fields, temperature, and voltage were performed with a simplified version of a model previously developed **[4]**. The simplified model is one dimensional in the radial direction. We expect that the one-dimensional approximation should be valid, since the current input is nearly axisymmetrical, the samples have a uniform diameter, and the part of the sample of interest is in the center region not too close to the electrode plates. To obtain the solutions, we solve numerically the coupled Maxwell and energy transport equations and then calculate the voltage from the computed results.

Let $\vec{B}$, $\vec{E}$, and $\vec{J}$ be the magnetic induction, the electric field intensity, and the current density, respectively. Let σ and μ be the electrical conductivity and the free space permeability, respectively. Then from Maxwell's curl equations and Ohm's law, we have

$$\nabla \times \vec{B} = \mu \vec{J}, \tag{3}$$

$$\nabla \times \vec{E} = -\frac{\partial \vec{B}}{\partial t}, \tag{4}$$

and

$$\vec{J} = \sigma \vec{E}. \tag{5}$$

From symmetry and the one-dimensional nature of the problem, we assume that $J_\theta = 0, E_\theta = 0, \vec{B} = B\hat{a}_\theta$ and that all the variables depend only on the radial coordinate r. With those assumptions, Equations (3) through (5) can be uncoupled to produce a single, second order,

partial differential equation that predicts the diffusion of the magnetic induction field. The result is

$$\mu\sigma\frac{\partial B}{\partial t}=\frac{\partial^2 B}{\partial r^2}-\frac{B}{r^2}+\frac{1}{r}\frac{\partial B}{\partial r}-\frac{1}{\sigma}\frac{\partial\sigma}{\partial r}\frac{\partial B}{\partial r}-\frac{B}{\sigma r}\frac{\partial\sigma}{\partial r}. \tag{6}$$

If we let e represent the internal energy of the sample, we have from energy conservation

$$\rho\frac{\partial e}{\partial t}=\kappa\frac{\partial^2 T}{\partial r^2}+\frac{\kappa}{r}\frac{\partial T}{\partial r}+\frac{\partial\kappa}{\partial r}\frac{\partial T}{\partial r}+\frac{1}{\mu^2\sigma}\left(\frac{\partial B}{\partial r}+\frac{B}{r}\right)^2. \tag{7}$$

In this equation, ρ represents the mass density, κ the thermal conductivity, and T the temperature. The last term on the right-hand side of Equation (7) represents the energy dissipated in the sample per unit volume and time because of ohmic heating, and the remaining terms correspond to local changes in the temperature that result from ordinary heat conduction. Generally, the last effect is negligible on the small time scale of interest here, but the effect is included nevertheless. The internal energy is related to the temperature through an equation of state, which we take to be

$$e=\int_0^T C(T)\,dT+H_F\Theta(T-T_m). \tag{8}$$

In this equation, C represents the specific heat, T_m is the melt temperature, H_F is the heat of fusion, and Θ is the Heaviside function given by zero when T is less than T_m, and given by unity when T is greater than T_m. In writing Equation (8), we have assumed that melting, the only phase change accounted for, occurs at a well-defined temperature T_m. We have also assumed that $e=0$ at $T=0$.

The thermodynamic and electrical properties (i.e., the density, specific heat, thermal conductivity, and resistivity η [=1/σ]) were represented by power series approximations of the form

$$F=\sum_j a_{S,L}(j)T^j, \tag{9}$$

in which F is any one of the properties and S or L denotes solid or liquid. For properties in which there is a discontinuous change in values at the melting temperature, the property in question was scaled linearly with energy e during the melting process, i.e., when the temperature is constant and equal to T_m. Values of $a_S(j)$ and $a_L(j)$ as well as the appropriate references are given in the appendix for molybdenum, tantalum, and tungsten.

Equations (6) and (7) must be solved, subject to the boundary conditions that the temperature gradient be zero at $r = 0$ and at $r = r_0$, in which r_0 is the radius of the sample. From Ampere's law, it also follows that $B\,(r = 0) = 0$ and

$$B(r=r_0)=\frac{\mu I}{2\pi r_0}, \tag{10}$$

in which I is the total pulsed current at time t. The value of I as a function of time is taken directly from the experimental data.

Once values of the electromagnetic fields have been obtained from the solution of the equations, the voltage corresponding to that actually measured can be calculated. To do so, we apply Stokes' theorem to Equation (4) to produce

$$\oint \vec{E} \bullet d\vec{\ell} = -\int \frac{\partial \vec{B}}{\partial t} \bullet d\vec{A}. \tag{11}$$

The integral on the right corresponds to an integral over the area enclosed by the voltage loop, and the integral on the left corresponds to a line integral along the loop. As pointed out previously, the loop always includes the outer surface of the sample and part of the area adjacent to it. Within that area, the induction field is given by $B = \mu I/(2\pi r)$, and along the surface of the sample, we have

$$E(r_0) = J(r_0)/\sigma(r_0) = \frac{1}{\sigma(r_0)}\left[\frac{1}{r}\frac{\partial}{\partial r}(rB)\right]_{r=r_0}. \tag{12}$$

Making these substitutions in Equation (11), we have for the "measured" voltage V_M the result

$$V_M = \ell J(r_0)/\sigma(r_0) + M_T \frac{dI}{dt}, \tag{13}$$

in which ℓ is the part of the sample across which the voltage is being measured and M_T is given by

$$M_T = \int\int \frac{\mu}{2\pi r} dA. \tag{14}$$

The first term on the right-hand side of Equation (13) can be recognized as the calculated resistive voltage Vr_T, referred to earlier, and the second term on the right-hand side refers to the calculated inductive voltage.

We have employed various voltage loops in the experimental measurements and, for each, the integral in Equation (14) must be computed. The two most commonly used loops are a loop with the shape shown in Figure 2 and one that is rectangular. The integrals are easy to evaluate. For the first loop, we have

$$M_T = \frac{\mu}{2\pi}\left\{\ell \log(r_1/r_0) + (z_2 - z_1)\log(r_2/r_1) + \frac{r_1(\ell + z_1 - z_2)}{r_2 - r_1}\left[\frac{r_2}{r_1}\log(r_2/r_1) - \frac{r_2}{r_1} + 1\right]\right\} \tag{15}$$

The rectangular loop is clearly just a special case of the one shown in the figure with $z_1 = z_2$ and $r_1 = r_2$. For that loop, only the first term in the braces is nonzero; the remaining terms can be shown to vanish.

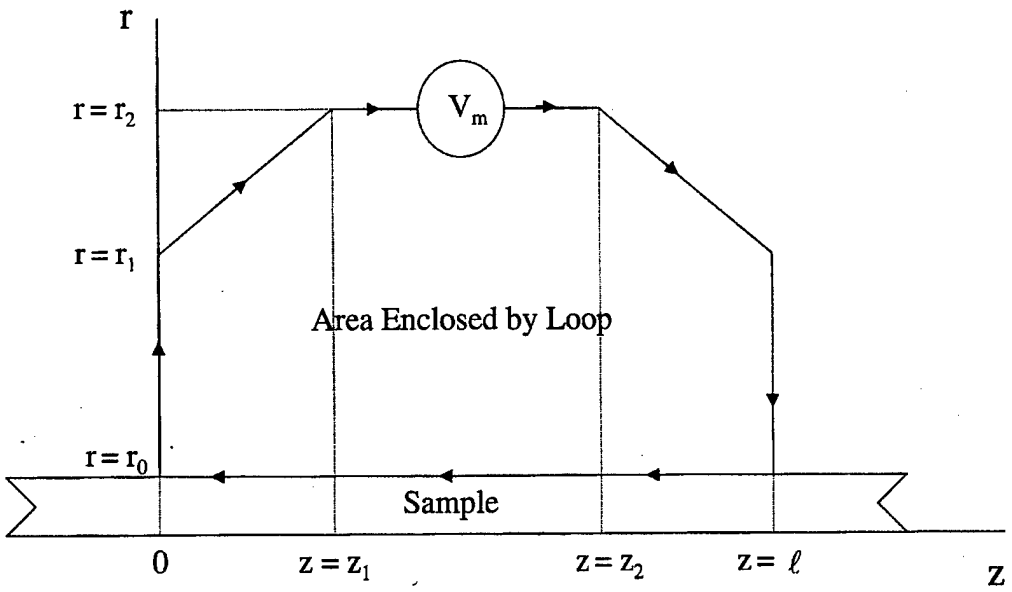

Figure 2. Typical loop employed for voltage measurements and calculations.

4. Results

4.1 Voltage Measurements

In this section, we present our results in terms of two measurements for each element, one for a relatively high temperature below the melting temperature for that element and one that extends into the region of melting. For molybdenum, we present one additional voltage measurement in Section 4.2 because it supplements the temperature measurements discussed there.

The potential for considerable systematic error exists because of the procedure used to determine the resistive voltage, i.e., subtraction of a non-negligible inductive component from the experimentally measured voltage. Because of current reversals and the steep slope of the voltage curves near zero current, it is necessary to restrict the region where theory and experiment are compared. We have arbitrarily chosen the region of comparison to be that contained between the points where the calculated resistive voltage is 0.707 times the peak calculated value. Section 4.1.1 shows that this procedure leaves only a very small data gap when the resistive voltage is plotted versus temperature.

The inductive voltage, in the absence of motion of the measurement loop, will follow the I-dot signal. It has a maximum value at the initiation of current and is much smaller, but not zero, at the peak of a typical resistive voltage curve. Therefore, we believe that the average deviation between calculated and derived experimental values of resistive voltage for all points in the range of comparison is a reasonable way to discuss agreement between theory and experiment.

We assume that the uncertainty in the theoretical predictions for voltage below the region of melt is determined by the approximately 3% uncertainties each in the resistivity and specific heat for this temperature range. For limited temperature regions, the error assigned to the evaluated data for a particular parameter and a particular element may be only 2%, but a value of 3% is a good representative number for all three elements below the region of melting. Some errors, such as those related to current and voltage measurements, are easy to assign. Others, however, are not. The error associated with the size of the measurement loop, i.e., the correct value of M, is an example of the latter situation for the following reasons.

The ratio of the inductive voltage to the resistive voltage decreases significantly with successive resistive peaks. The time derivative of the current, proportional to the inductive voltage, decreases much more rapidly with time than does the current, whose squared values are related to heating and the resistive voltage. For example, for tantalum and tungsten and where the melt condition is realized, the ratio of inductive to resistive voltage at the first peak is about 0.18; at the second peak, the ratio has dropped to 0.01 or less (these estimates assume the rectangular flux loop described in Section 3). Moreover, the relative importance of this effect for a given resistive peak depends on the resistivity of the material. Considering all the known sources of error, we believe that our results are accurate to about 10% in regions where the thermophysical parameters are assumed to be known to about 3% each. This accuracy applies to the average deviations observed over a particular temperature range and not to individual point-by-point data for the reasons just given.

4.1.1 Molybdenum

The initial setups and experimental runs were done with molybdenum samples; this work included a number of tests at low charge voltages to determine probable errors and the limits of the experimental technique. Most of the data were acquired with one of the two flux-loop configurations discussed in Section 3. However, some early runs were made with a large loop that included the entire region between the electrodes except for a 25 mm × 25.4 mm rectangle extending from the surface of the sample to each electrode (see Figure 1). In other words, the voltage leads extended vertically 25.4 mm from the sample surface and then ran parallel to the rod until they exited the electrodes. This loop has an inductance of about 66 nano-henrys (nH). This value leads to inductive voltages with magnitudes more than twice those of the calculated resistive voltage at the peak in resistive voltage. Nevertheless, as shown in Figure 3, the agreement between theory and experiment is within experimental error. The deviation, D, in percent, plotted in Figure 3(b) is defined by the following equation

$$D = 100\ (Vr_E - Vr_T)/\ Vr_T \qquad (16)$$

in which Vr_E is the deduced resistive voltage, defined in Equation (1), and Vr_T is the calculated resistive voltage, discussed in Section 3. As noted in Section 4.1, we plot deviations only for those points that fall within the range described in Section 4.1.

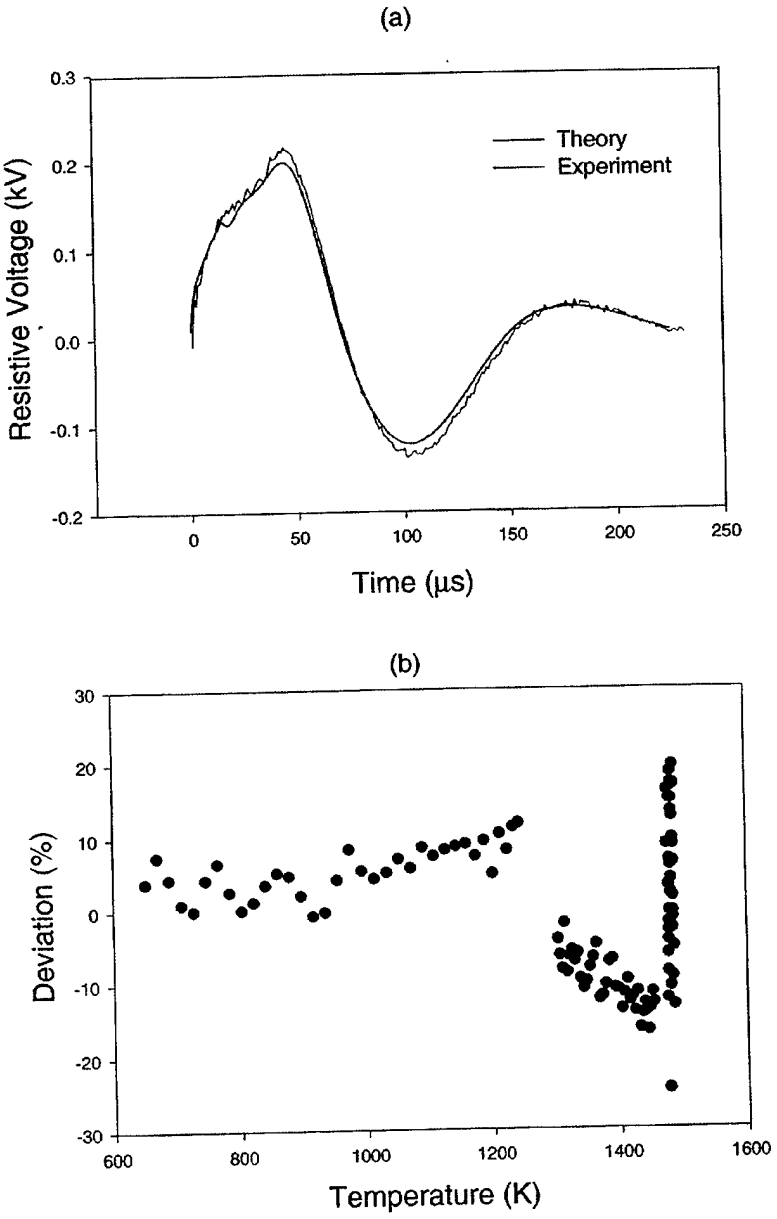

Figure 3. Results for molybdenum below the melting temperature: (a) surface resistive voltages, calculated and determined from experiment; (b) deviation between theory and experiment. (The average deviations for the first, second, and third peaks are +7.1%, -10.0%, and +3.2%, respectively.)

Our procedure is most useful for poor conductors with low thermal capacities because they produce large resistive voltages. Thus, molybdenum is the most difficult of the three elements studied to heat electrically to high temperatures. The 5.0 mm diameter molybdenum samples could not be heated to surface temperatures above 1600 K because of the voltage limitations of our switch. One molybdenum sample was machined to give an average diameter of 4.1 mm in order to obtain data at higher temperatures. The machining operation is not expected to change any of the thermophysical properties of the sample, but surface irregularities are undoubtedly more pronounced with this sample than with the others.

Figure 4 shows results for the 4.1 mm diameter molybdenum sample obtained with the rectangular loop, discussed in Section 3, at a charge voltage of 9.42 kV. Again, the deviations are within the estimated experimental error except in the region near where melting occurs, i.e., at 2894 K. The peak heating rate calculated for this run is 115×10^6 K/s, as shown in Figure 5. The evaluated parameters for molybdenum do not change much in the region above melting temperature, although the assigned errors increase to about 5%. The heating rate curve shows a transition back to a shape similar to that of the original curve following completion of sample melt. The maximum surface temperature calculated was 3341 K.

Naturally, the sample is destroyed in an event such as this; a video monitor showed that this sample exploded into innumerable hot fragments after the test. Even in less destructive runs (e.g., where the sample is heated to temperatures above 2000 K but below melting temperature), voltage contact appears to be maintained throughout the duration of the measurement, although the spring clips attached to the sample may be destroyed. In other words, there are no obvious irregularities in either of the two voltage signals.

We are unable to explain one feature of the resistive voltage curve of Figure 4(a), namely, the disagreement between theory and experiment near zero time. It most resembles a contribution from a dL/dt, i.e., motion of the loop. However, if it represented a permanent change in the loop area, or inductance, it should exhibit a more pronounced effect in the region of the voltage zero. In some tests, one spring clip of the measurement loop was loosely attached, and the same end was completely detached upon completion of the experiment. The effect on the experimental resistive voltage was dramatic: strong disagreement at early times accompanied by a significant shift in the peak location for the resistive voltage and very pronounced disagreement in its time of zero crossing. This result suggests that, for the period of interest, no appreciable extraneous contribution to the loop inductance existed.

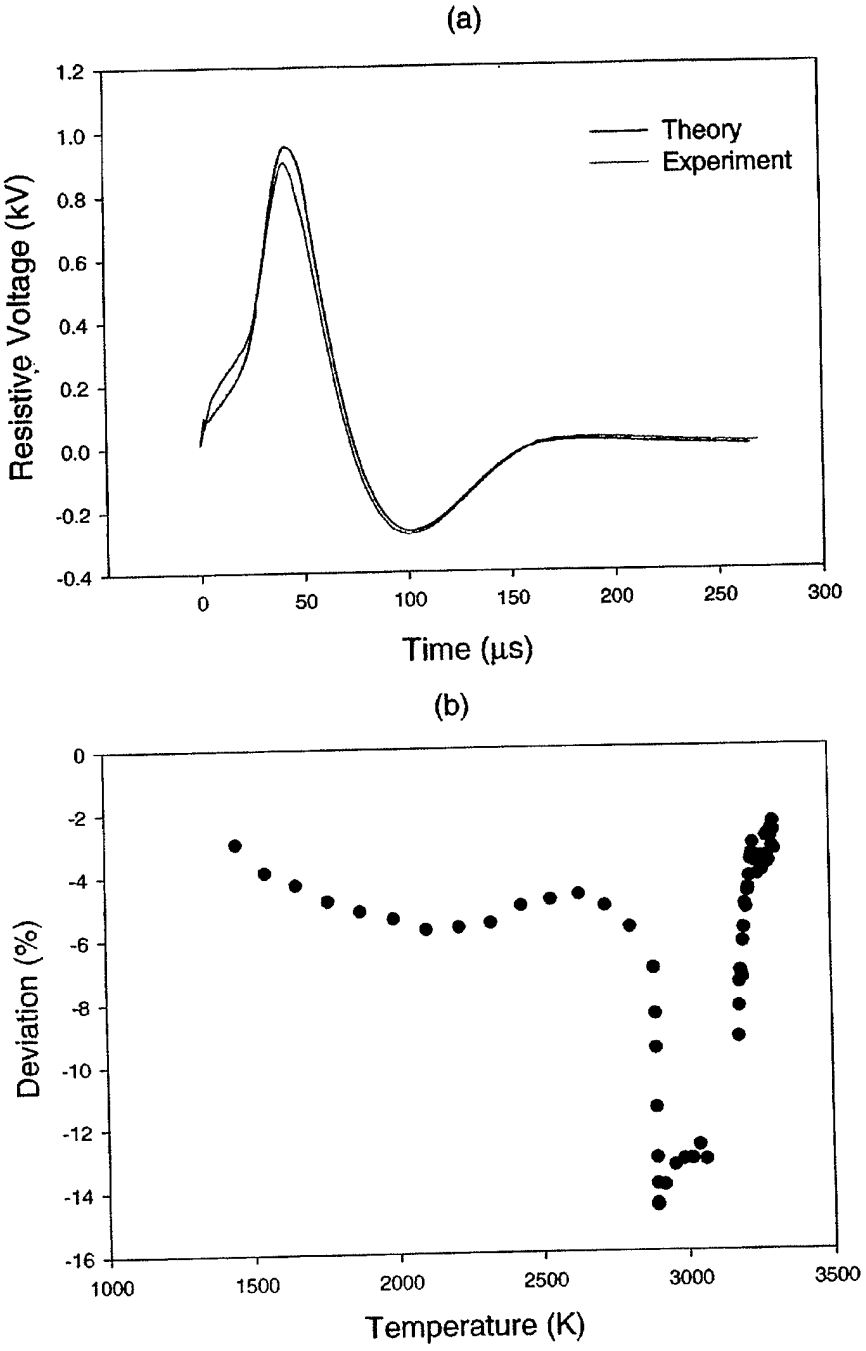

Figure 4. Results for molybdenum into the region of melting: (a) surface resistive voltages, calculated and determined from experiment; (b) deviation between theory and experiment. (The average deviations for the first and second peaks are –8.9% and –4.6%, respectively.)

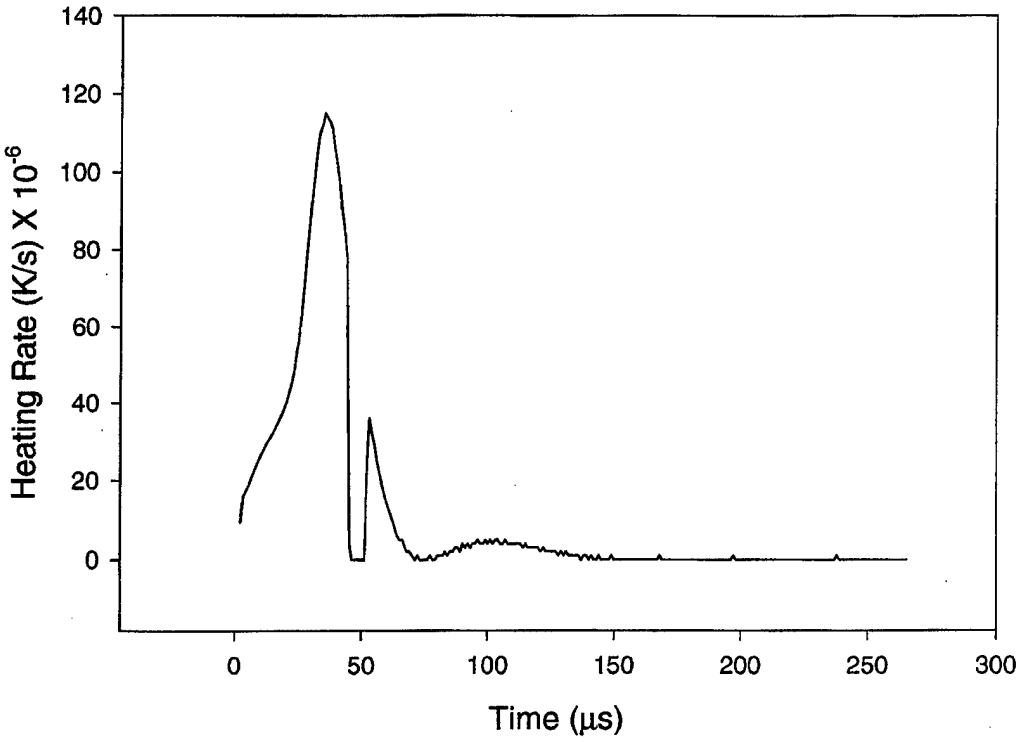

Figure 5. Surface heating rate for molybdenum into the melting region.

4.1.2 Tantalum

Data for a 5.0 mm diameter tantalum sample at a charge voltage of 8.01 kV, with the flux loop of Figure 2, are shown in Figure 6. The agreement between the calculated and experimentally determined voltage is very good throughout the entire temperature range. The maximum surface temperature predicted is 2279 K. The calculated maximum heating rate is 51×10^6 K/s, whereas the maximum surface current density is 1.6×10^{10} A/m^2.

The accumulation of reasonable data in experiments that culminated in the destruction of both the sample and the loop apparatus encouraged us to attempt some measurements with an approximately "zero flux" configuration. The stripped ends of enameled magnet wires were attached with conducting adhesive to the circumference of the sample at the desired separation. The wires were then glued to the sample surface and twisted together at the center of the region selected for measurement. They emerged from the electrode region as a twisted pair to the voltage probes. This procedure provides two layers of non-conducting materials that must be burned through, an epoxy layer and the enamel, before a portion of the measurement length could be "shorted" by contact between the magnet wire and sample surface. Experience proved that this technique worked reasonably well. The procedure, however, leads to an increased uncertainty in the effective length of the sample. The stripped wires could not be easily attached at the same position along the circumference of the wire; thus, a range of sample lengths existed.

The average values between the measured maximum and minimum lengths were used in the calculations.

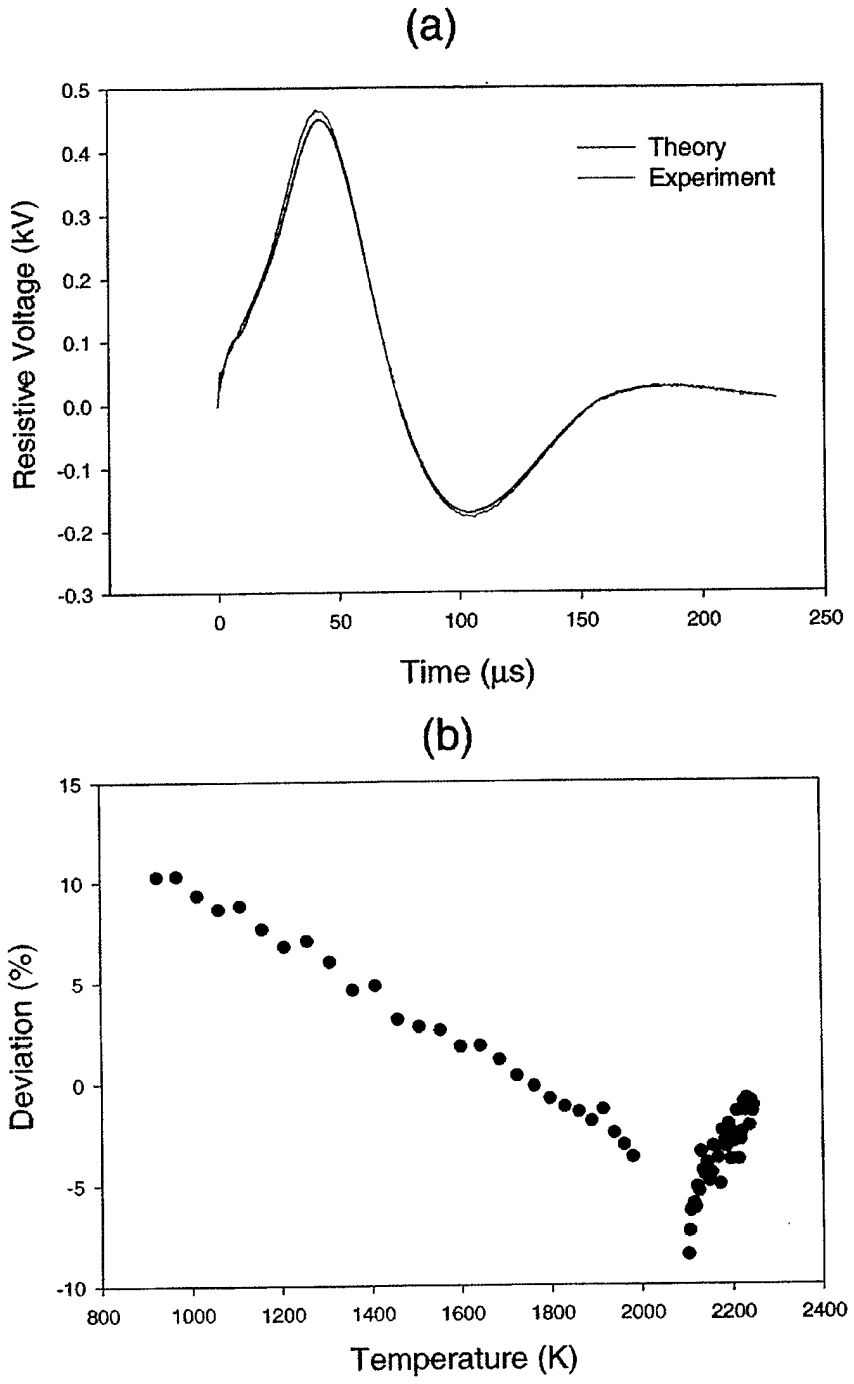

Figure 6. Results for tantalum below the melting temperature: (a) surface resistive voltages, calculated and determined from experiment; (b) deviation between theory and experiment. (The average deviations for the first and second peaks are +3.0% and –3.6%, respectively.)

The results of a "zero flux" run for a 5 mm tantalum sample at 9.24 kV are shown in Figure 7. The experimental voltage, i.e., the total measured voltage, is approximately zero at current initiation. That is, the experimentally measured voltage looks identical to the calculated resistive voltage. Thus, the conditions of "zero flux" loop are very nearly achieved in this case.

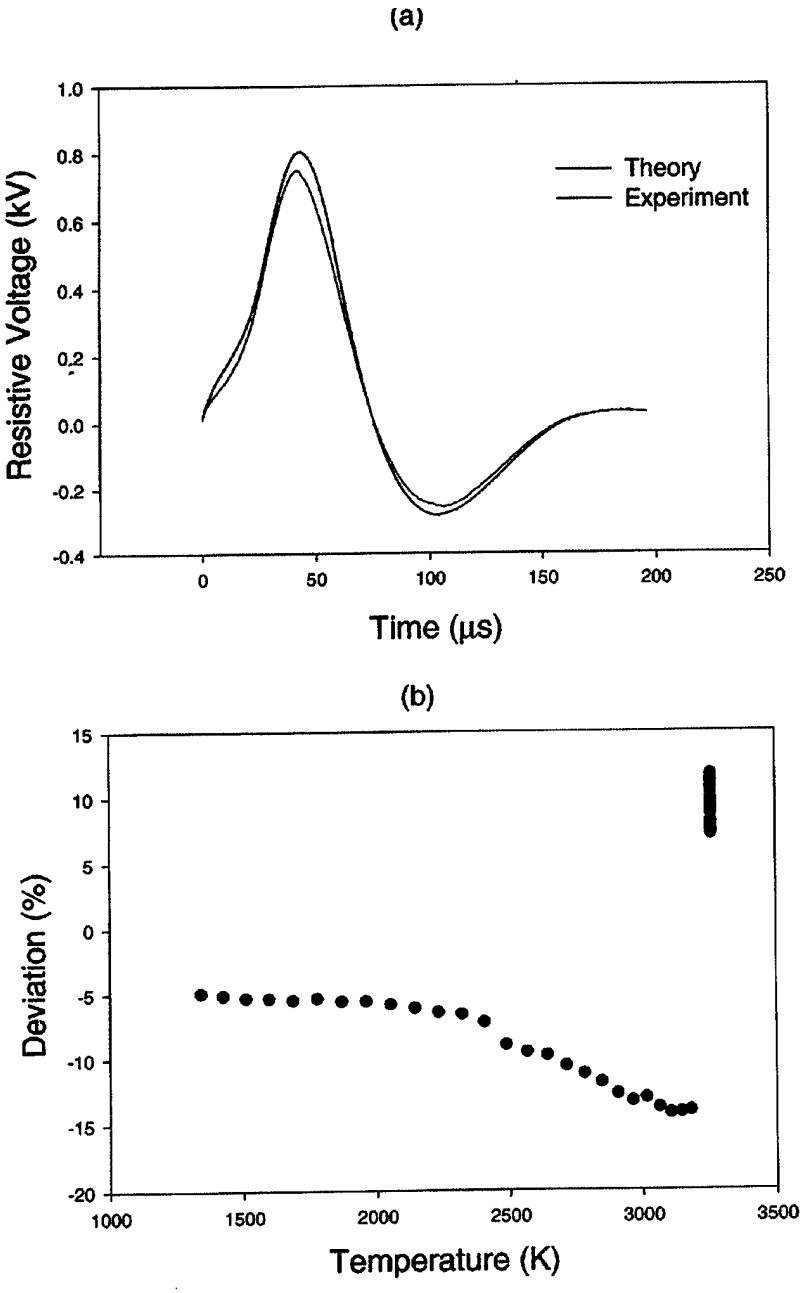

Figure 7. Results for tantalum into the region of melting: (a) surface resistive voltages, calculated and determined from experiment; (b) deviation between theory and experiment. (The average deviations for the first and second peaks are –9.2% and +9.7%, respectively.)

Our time resolution of 1 μs renders the voltage measurement at $t = 0$ unreliable. Otherwise, one could estimate the inductance by dividing the experimental voltage at zero time by the derivative of the current. Such a procedure implies zero current and no resistive voltage drop. A better approach follows.

The first few points, to 5 or 6 μs, can verify the calculated or estimated value of inductance. In this region, any inductive voltage is large, whereas the resistive voltage is small because of the small current and low resistivity. The calculated resistive voltage is then subtracted from the measured voltage and the result is divided by the derivative of the current to obtain the inductance. Even if the calculated value is erroneous, its effect in a corrective term can be small, particularly for large loops. This procedure worked reasonably well for all situations but in most cases was used only to confirm the inductance calculation. Unless otherwise stated, we used the calculated value of inductance to compare theory and experiment.

In the present case, the estimated "zero flux' inductance is 0.75 nH. For this particular tantalum run, the deviations and conclusions are not impacted significantly by the choice of either 0.0 or 0.75 nH for the inductance. The deviations shown in Figure 7 are based on the assumption that the inductance is zero.

4.1.3 Tungsten

The data for a 4.0 mm diameter tungsten sample at a charge voltage of 7.02 kV are shown in Figure 8. The flux loop is shown in Figure 2. While the data show some deviations outside the 10% range, the average deviations are within the limits of our estimated errors. The final surface temperature was 2148 K, and the peak current density was 2.2×10^{10} A/m^2 for this test.

The results of a "zero-flux" loop test for a 4.0 mm sample at a charge voltage of 8.63 kV are shown in Figure 9(a). The experimentally measured voltage at $t = 0$ showed a small step, which was indicative of an existing small inductance in the circuit. Thus, the resistive voltage of Figure 9(a) was obtained by subtraction of an inductive voltage component from the measured voltage. This residual inductance, estimated by the method described previously, is 4.5 nH.

Although the average deviations are within the acceptable range of errors, more pronounced systematic trends are evident for this measurement than for any of the others. This result is not unexpected. Appreciable uncertainty exists regarding the thermophysical parameters for tungsten near and at the melting temperature. The evaluated data set for resistivity ends at 3400 K, about 260 K below the melting temperature. According to the evaluators, the data are too uncertain to assign values for higher temperatures. It is known that the specific heat increases significantly at the transition point, but the exact amount is not well known. For example, two of the experiments frequently referenced for these data **[7,8]** report values that disagree by more than 30% at 3600 K. Dikhter and Lebedev **[7]** estimate the error to be greater than 10% in the temperature range 3600 to 3720 K, and they do not present any data there, although they present data for still higher temperatures.

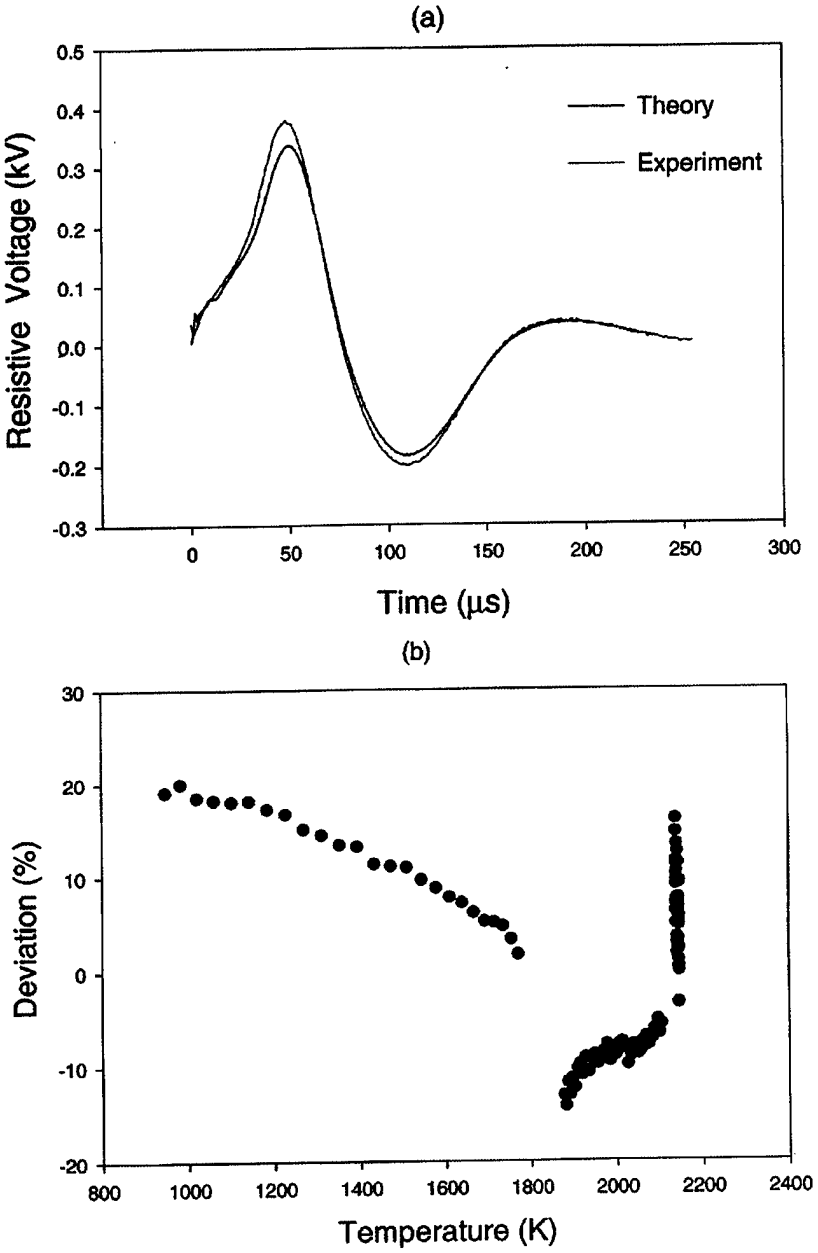

Figure 8. Results for tungsten below the melting temperature: (a) surface resistive voltages, calculated and determined from experiment; (b) deviation between theory and experiment. (The average deviations for the first, second, and third peaks are +11.8%, -8.9%, and +6.2%, respectively.)

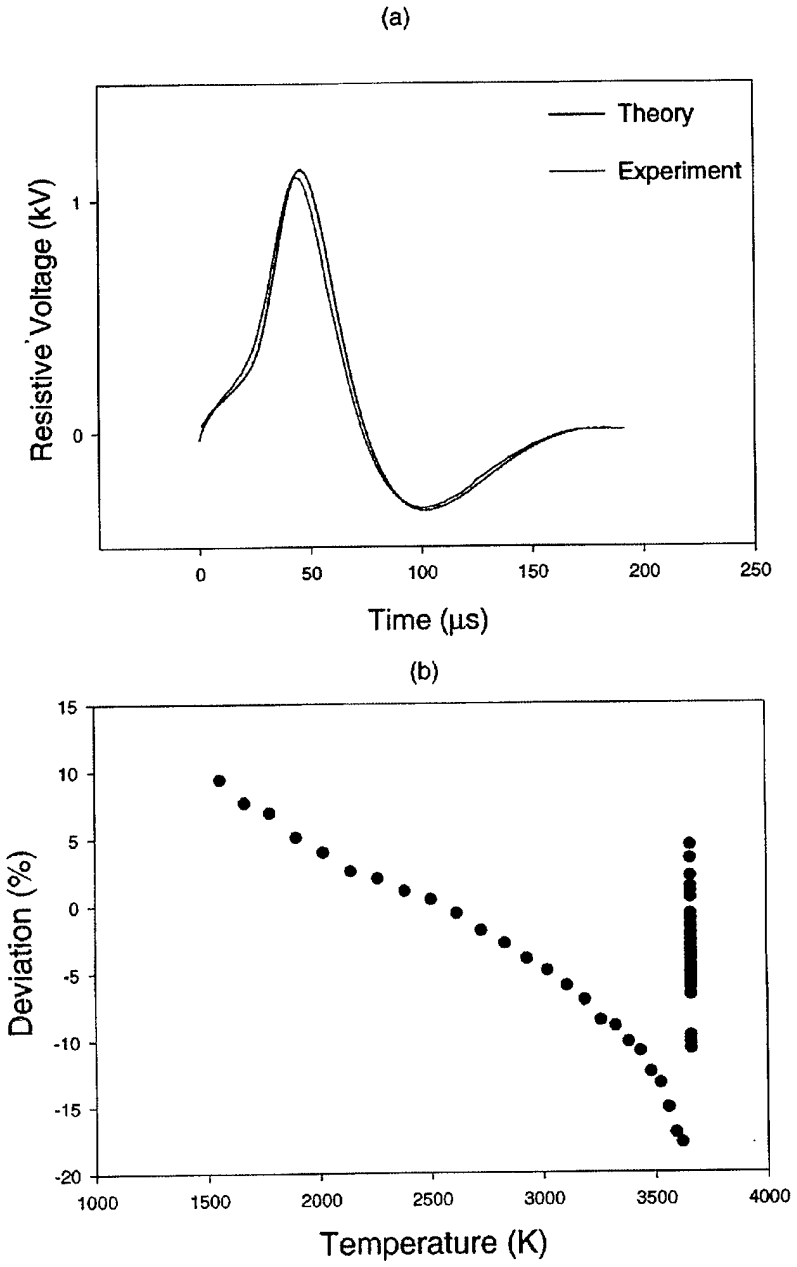

Figure 9. Results for tungsten into the region of melting: (a) surface resistive voltages, calculated and determined from experiment; (b) deviation between theory and experiment. (The average deviations for the first and second peaks are –4.3% and –9.3%, respectively.)

In our theoretical calculations, we used the polynomial that describes the evaluated data for resistivity below 3400 K to predict values throughout the solid phase. For the specific heat at melting, we used the average of the values quoted in References **[7]** and **[8]**. Our errors can be expected to be very large in this region.

4.2 Temperature Measurements

The electrode assembly in Figure 1 was not designed with temperature measurements in mind, i.e., the sample contact points are not shielded from the camera whose view encompasses the entire region between the electrodes. Initiation of current flow in the sample is accompanied by the production of electrical arcs in the vicinity of the test stand, particularly at contact points. Copious quantities of visible light, to which the Flashcam is particularly sensitive, are produced. These emissions may reflect directly from the sample surface or indirectly from the surfaces of the aluminum electrodes and may contribute to the observed signal level. Detectors in the CCD array also could be saturated by arc emissions, a situation that could produce errors because of uncertainties in the recovery time of the detectors. Thus, it is necessary to avoid data accumulation until the initial illumination has decayed and the detectors have recovered.

By observing a series of images of decaying arcs when molybdenum rods were heated electrically, we determined that a 50 ms delay was more than adequate to ensure that the arc light did not affect the images of the thermal emission from the rod. For all the tests involving the capture of a single image, the camera was triggered 50 ms after the pulse and a total integration time of 10 ms (ten 1-ms exposures) was used. The measured cooling rate of 10 K/s implies that sample temperature drops only 0.5 K during the 50 ms delay; thus, no correction for cooling is necessary.

For molybdenum, three runs were made with pre-oxidized samples at a charge voltage of approximately 7.5 kV. A plot of the circuit current that was used to heat the sample in Shot S1 is shown in Figure 10(a); the calculated surface temperature of the sample as a function of time for this shot is shown in Figure 10(b).

As noted previously, the camera was calibrated in both the triggered and free-run modes of operation and both were used in the experiments. In Figure 11, the Flashcam image of the molybdenum rod from Shot S1 is shown; in Figure 12, the digitized Flashcam output for all three shots is shown. Also shown in Figure 12 are three calibration curves that indicate the temperature to be associated with a given signal amplitude. The horizontal position of the calibration curves in this graph has been arbitrarily shifted for clarity of presentation. All data, both calibration and experiment, were obtained for the following conditions: (1) f-number of 0.85, (2) 10 successive 1 ms exposures, and (3) a lens-to-sample distance of 650 mm.

The results for three separate temperature measurements for molybdenum and the corresponding theoretical predictions are compared in Table 1. The predictions were obtained with the model discussed previously and with the experimentally measured current used as input. The differences between the theoretical and experimental results are well within the experimental uncertainty, but because of the limited number of tests, they do not reflect the normal spread of differences.

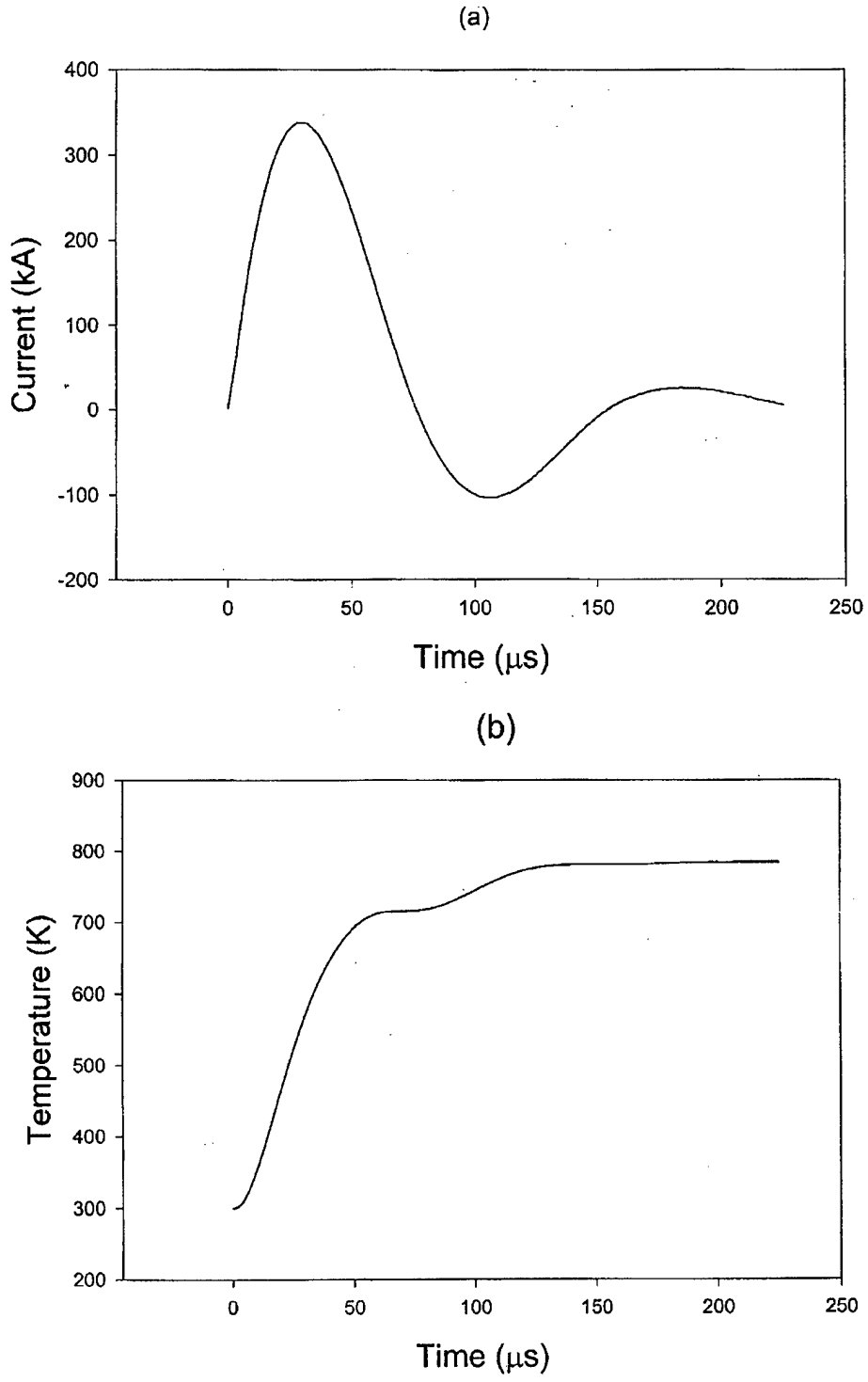

Figure 10. Data for molybdenum at a charge voltage of 7.51 kV:
(a) current trace; (b) temperature of sample.

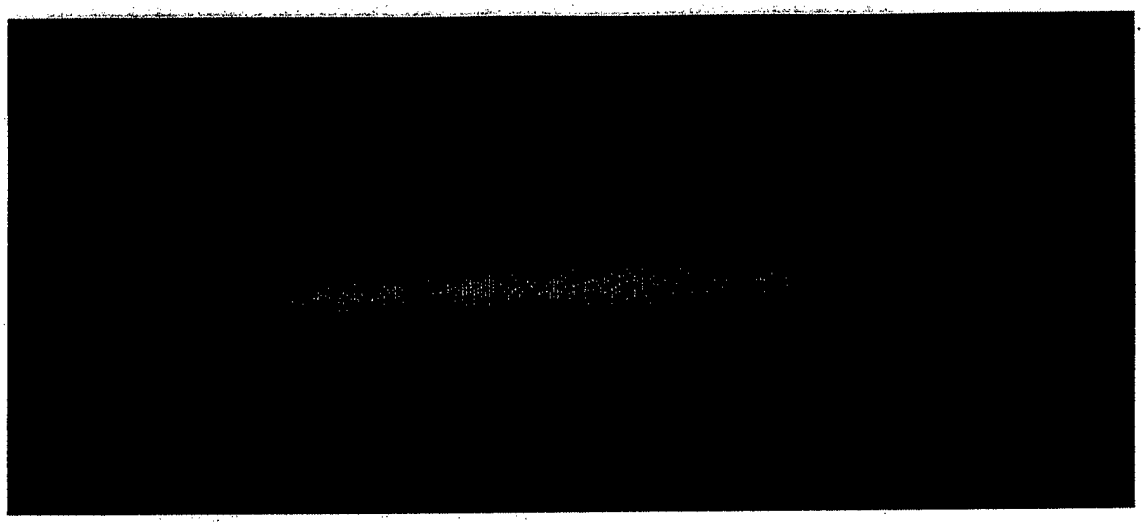

Figure 11. Flashcam image of pulse heated molybdenum rod.

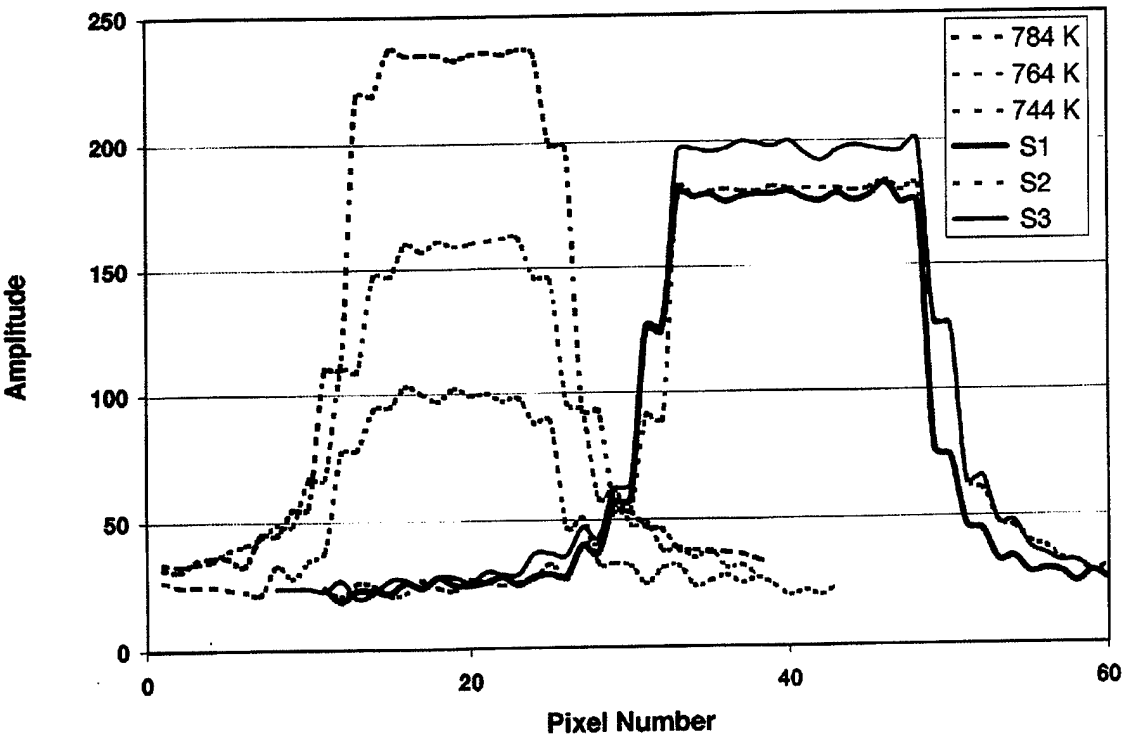

Figure 12. Profiles of surface temperature video levels of pulse heated rods versus calibration curves.

Table 1. Comparison of the calculated and measured temperatures for molybdenum (all results are in degrees Kelvin)

Shot Number	Theory (*K*)	Experiment (*K*)	Difference (*K*)
S1	774	770	- 4
S2	776	772	- 4
S3	777	774	- 3

One measurement each was made for the tantalum and tungsten samples; the results are shown in Table 2. Only the measured temperature for the tantalum sample falls outside the range of values permitted by the ±20 K uncertainty in our measurement; it is, however, well within the range of the predicted values if the uncertainties in the specific heat and resistivity are taken into consideration.

Table 2. Comparison of the calculated and measured temperatures for tantalum and tungsten (all results are in degrees kelvin)

Sample	Theory (*K*)	Experiment (*K*)	Difference (*K*)
Tantalum	761	728	-33
Tungsten	769	783	+14

Because of the oxide or paint coating on the surface of the samples, it was not practical to take voltage measurements at the same time that the temperature measurements were made. Throughout all the experiments, the reproducibility of experimental conditions was very good, i.e., the same charge voltage repeatedly produced the same peak current. This behavior is partly attributable to the fact that the power source contains a rather large constant resistance associated with the energy-absorbing resistors attached to each capacitor. Therefore, we do not believe that any loss in generality is associated with separate measurements of temperature and voltage. The results of a voltage measurement for molybdenum at a charge voltage of 7.52 kV are shown in Figure 13. The flux loop was that shown in Figure 2. These data show clearly the effects of the larger ratio of inductive to resistive voltage at lower charge voltages; fluctuations not normally visible in most of the other data taken at higher charge voltages are apparent in this data set.

5. An Iterative Technique for Determining Resistivity as a Function of Temperature

In the previous section, we confined our attention to comparing theoretical and experimental results obtained for conductors whose properties are well known. However, one of the principal objectives of this work, and one that will occupy most of our future efforts, is to determine properties of materials of Army interest when those properties are not known *a priori*. For this purpose, we have developed a technique that couples theory and experiment in such a way that we can determine resistivity as a function of temperature from a single pulsed heating experiment followed by a short calculation. Therefore, we avoid the difficult and time-consuming effort involved with point-by-point measurements. In this section, we describe the procedure and illustrate its application in the determination of the resistivity of tantalum. Other materials, such as various alloys whose resistivity is not known, will be investigated in future work.

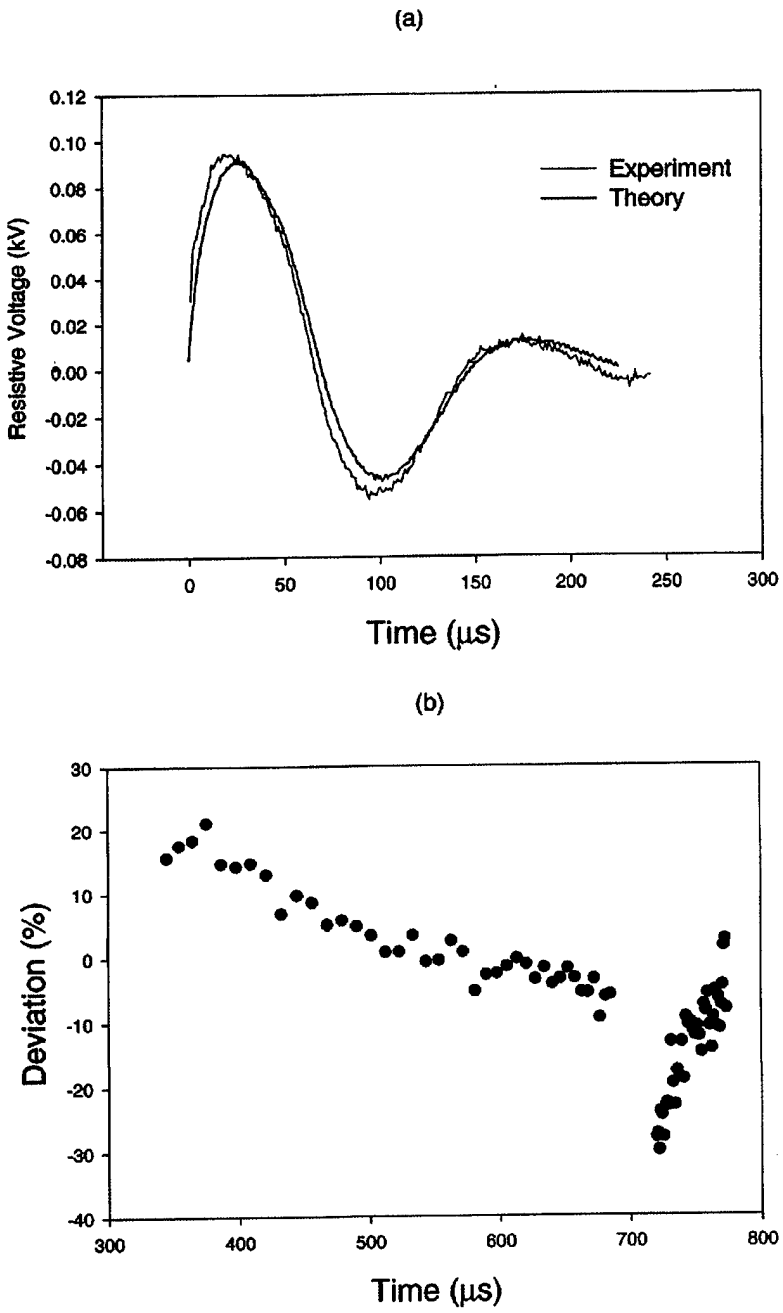

Figure 13. Results for molybdenum at 7.5 kv: (a) surface resistive voltages, calculated and determined from experiment; (b) deviation between theory and experiment. (The average deviations for the first and second peaks are –0.1% and -9.9%, respectively.)

The procedure is based on an assumption that the specific heat for the substance being studied is known or can be constructed from knowledge of the atomic composition. Usually, this determination is not difficult and produces reasonably accurate results for bulk properties such as

the specific heat. Similarly, it is assumed that the thermal conductivity is known or, more likely, is unimportant because the time scale on which the measurements are made is too small for thermal conduction to be important; very approximate values then are satisfactory for use in the calculations.

The procedure is performed in the following steps. First, a resistivity versus temperature profile for the material in question is assumed. For example, for an alloy, we might assume the resistivity of the dominant element if that functional relationship is known. The assumed resistivity η_A is represented as a polynomial in T, namely,

$$\eta_A = \sum_j C_{A,j} T^j . \tag{17}$$

Usually, a linear fit is found to be satisfactory as an initial guess. Second, the sample is subjected to pulsed heating in the same manner as previously, and the current and voltage are measured as a function of time. Third, a calculation is performed with the model described in Section 3. The experimental values of $I(t)$ are used in the calculation as well as the assumed resistivity η_A. Instead of calculating a voltage V_M, however, we use the experimental values and calculate from Equation (13) a new resistivity η at selected points in time during the discharge. Furthermore, since we also calculate the temperature, we can construct a new curve of η versus T. These new values are then fit by a least squares method to a new polynomial similar to that in Equation (17). Of course, the coefficients in the polynomial are not the same as the initially assumed values.

It is evident, however, that the new curve $\eta(T)$ does not adequately represent the resistivity, since the temperature was calculated with the assumed, not the correct, resistivity. Consequently, it is necessary to replace the assumed resistivity with the new resistivity (actually a weighted average of the two works best) and to repeat the calculation until convergence is obtained. Typically, reasonable convergence is obtained in a few tens of iterations.

We demonstrate the procedure via a determination of the resistivity of tantalum in the temperature range from 300 to about 2100 K. We assumed as an initial (and wrong) guess a linear function for the resistivity with a slope that was sufficiently large that the assumed values of η were somewhat greater than the "handbook" values (see Figure 14). The room temperature value was assumed to be known accurately, since this value is easily obtained with a single measurement. The calculation was then performed as just described, with the values of η versus T being fit to a quadratic in successive iterations. After 65 iterations, we found that the coefficients in the quadratic (i.e., C_0, C_1, and C_2) had converged to within one part in 10^5. The resulting curve, also shown in Figure 14, is obviously in very good agreement with the curve that represents the handbook values.

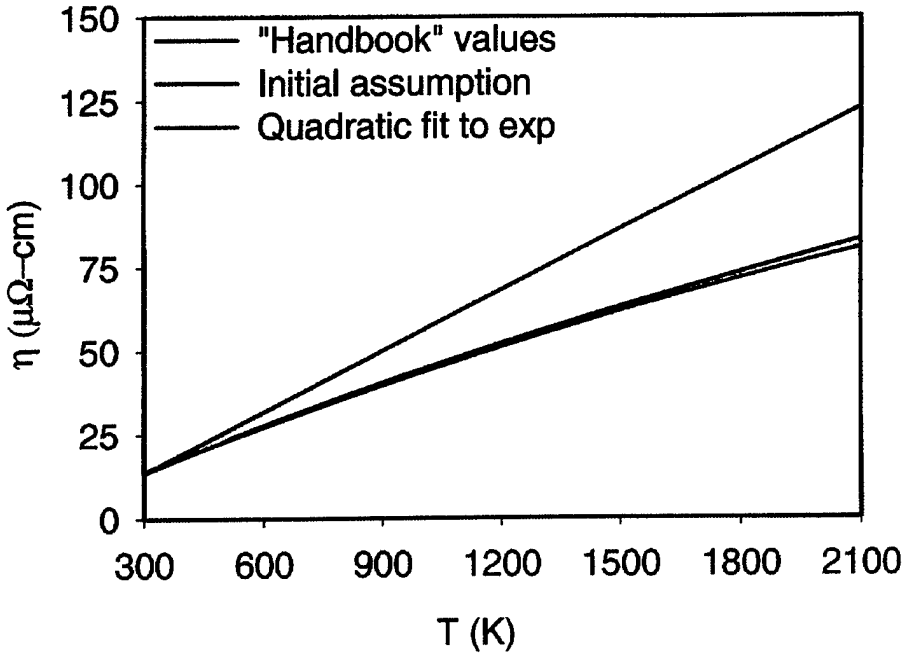

Figure 14. Resistivity of tantalum obtained via iterative technique.

6. Summary, Conclusions, and Future Work

Measurements of surface heating in millimeter-diameter rods of molybdenum, tantalum, and tungsten have been made in two temperature ranges, one below the melting temperature and one into the region of melting. Pulsed currents of several hundred kilo-amperes were used. The time-dependent voltage across a fixed length along the surface of the sample was measured experimentally and compared with the voltage calculated with a one-dimensional computer code that couples the transport of electromagnetic fields and energy within the conductor.

The agreement between the calculated and experimentally measured voltages was remarkable throughout the entire temperature range for all three samples studied. In addition, good agreement between theory and experiment was found for measurements of the final surface temperature that were made on samples heated to about 800 K. Since the thermophysical properties of these samples are known very accurately as a function of temperature, the good agreement between theory and experiment lends credence to our experimental measurements and to the validity of our numerical calculations. The agreement also allows us to infer an absence of heating rate effects on the thermophysical properties despite the high current densities (on the order of 3×10^{10} A/m^2) and high surface heating rates (on the order of 10^8 K/s), which were present in the experiments.

The techniques reported herein have also been applied to other materials, including some relatively good conductors, e.g., several aluminum alloys of interest for various applications. The results were unsatisfactory for materials that have low resistivity and high thermal capacity. For these materials, the resistive component of the voltage is very small when compared to the inductive component, even for our small inductive loops. Consequently, subtracting the inductive voltage from the measured voltage (two large numbers) to obtain the resistive voltage (a small number) can lead to significant errors. This problem could be ameliorated in future work by reconfiguring the power supply as a pulse-forming network, or PFN. These networks can be designed to produce a relatively rapid initial rise in current, followed by a long period of almost constant current. Thus, after the initial rise in current, the inductive voltage, which depends on the derivative of the current, can be reduced to a negligible level. Consequently, the accuracy of the measurements can be increased significantly. In addition, the iterative procedure, described in Section 5, would have application to a much greater variety of materials, including good conductors with high heat capacity.

It would also be worthwhile in future work to employ more accurate techniques for temperature measurements. Many options and alternate techniques, not exercised in the present experiment, could be used to extend the range of temperature measurements with video thermography. Broadband spectral techniques, such as those used in the present experiment, will always offer more potential for high speed imaging than will narrowband techniques, because more photons are collected. However, the use of narrow spectral band filters, possible at the radiances associated with higher temperatures, could also be a useful tool in some situations, e.g., as a means of reducing extraneous arc light or to improve accuracy. A two-color thermometry technique, based on the ratio of spectral radiance in two bands **[9]** may also offer advantages for high temperature measurements.

References

1. Cezairliyan, A., *Compendium of Thermophysical Property Measurement Methods*, Vol. 1, In K.D. Maglic, A. Cezairliyan, V.E. Peletshii, Eds., pp.643-668, Plenum, New York, NY, 1984.

2. Cezairliyan A., *Compendium of Thermophysical Property Measurement Methods*, Vol. 2, In K.D. Maglic, A. Cezairliyan, V.E. Peletshii, Eds., pp.483-517, Plenum, New York, NY, 1992).

3. Kaschnitz, E., and P. Reiter, "Thermophysical Properties of Solid and Liquid 90Ti-6Al-4V in the Temperature Range 1400 to 2300 *K* Measured by Millisecond and Microsecond Pulse-Heating Techniques," *Fourteenth Symposium on Thermophysical Properties*, National Institute of Standards and Technology, Boulder CO, June 25-30, 2000.

4. Powell, J.D., *Current and Heat Transport in Axisymmetric Conductors*, ARL-TR-2066, U.S. Army Research Laboratory, Aberdeen Proving Ground, MD, 1999.

5. Ford, R.D., G. Dorr, R. Reams, and A.J. Toepfer, "High-Coulomb Triggered Vacuum Flashover Switch", *11th IEEE International Pulsed Power Conference,*" IEEE Catalog No. 97CH36127, Vol. II, p. 893, Baltimore MD, 1999.

6. Hollandsworth, C.E., C.R. Stumpfel, J.D. Powell, and C.R. Hummer, *A Video Thermography Technique for Temperature Measurements of Pulse-Heated Metallic Rods*, ARL-TR-2420, U.S. Army Research Laboratory, Aberdeen Proving Ground, MD, 2001.

7. Dikhter, I. Ya, and S.V. Lebedev, "Measurement of the Specific Heat and the Heat of Fusion of Tungsten at High Temperatures by the Wire Explosion Technique," *High Temperatures-High Pressures*, Vol 2, pp. 55-58, 1970.

8. Kraftmakher, Ya. A., in collected papers *Investigation in High Temperatures*, Nauka, Novosibirsk, 1966.

9. Zielinski, A.E., S. Niles, and J.D. Powell. "Current and Heat Transport During a Pulsed Electrical Discharge," *Journal of Applied Physics*, Vol. 86, p.4933, 1999.

Appendix A: Thermophysical Properties of Molybdenum, Tantalum, and Tungsten

In this appendix, we present the melting temperatures, latent heats, and coefficients that appear in the power-series expansions for the various thermophysical properties of molybdenum, tantalum, and tungsten. It should be recalled that any property F (i.e., C, η, κ, or ρ) is represented in the form

$$F = \sum_j a_{S,L}(j) T^j, \tag{A-1}$$

in which $a_{S,L}(j)$ denotes the coefficient in question. All coefficients are in the appropriate SI units. The data are presented in Tables A-1, A-2, and A-3.

Table A-1. Thermophysical properties of molybdenum

$T_M = 2894\ K$				
$H_F = 2.5 \times 10^5\ J/(kgK)$				
Coefficient	$C\ (J/kgK)$	$\eta\ (\Omega\text{-}m)$	$\kappa\ (W/mK)$	$\rho\ (kg/m^3)$
a_S (-3)	0	0	3.16906×10^{9}	0
a_S (-2)	0	0	-2.67950×10^{7}	0
a_S (-1)	0	0	7.85718×10^{4}	0
a_S (0)	2.22592×10^{2}	-1.70210×10^{-8}	5.56400×10^{1}	1.02300×10^{4}
a_S (1)	1.12500×10^{-1}	2.33190×10^{-10}	0	0
a_S (2)	-5.82479×10^{-5}	2.55070×10^{-14}	0	0
a_S (3)	2.04604×10^{-8}	-2.59300×10^{-18}	0	0
a_L (0)	6.08300×10^{2}	9.70000×10^{-7}	7.97213×10^{1}	1.02300×10^{4}

The evaluated data sets of Desai, Chu, and Ho[1] or White and Collocott[2] were used to provide resistivity data for all three elements. If the authors provided a polynomial fit to the evaluated data set, we used their coefficients. If no such fit was provided, we derived one that represented the tabulated data.

[1] Desai, P.D., T.K. Chu, and C.Y. Ho, "Electrical Resistivity of Selected Elements," *Journal of Physical Chemistry*, reference data, Vol. 13, No. 4, pp.1069-1096, 1984.

[2] White, G.K., and S.J. Collocott, "Thermophysical Properties of Some Key Solids," *International Journal of Thermophysics*, Vol. 18, No. 5, 1997.

Table A-2. Thermophysical properties of tantalum

$T_M = 3258\ K$				
$H_F = 1.74 \times 10^5\ J/(kgK)$				
Coefficient	$C\ (J/kgK)$	$\eta\ (\Omega\text{-}m)$	$\kappa\ (W/mK)$	$\rho\ (kg/m^3)$
$a_S\ (0)$	1.32235×10^{2}	-1.67790×10^{-8}	5.64800×10^{1}	1.66000×10^{4}
$a_S\ (1)$	2.26065×10^{-2}	5.31000×10^{-10}	3.07650×10^{-3}	0
$a_S\ (2)$	-2.35768×10^{-6}	-8.44510×10^{-14}	9.06800×10^{-7}	0
$a_S\ (3)$	0	1.15290×10^{-17}	-2.73310×10^{-10}	0
$a_L\ (0)$	1.80862×10^{2}	1.30000×10^{-6}	6.66769×10^{1}	1.66000×10^{4}

Table A-3. Thermophysical properties of tungsten

$T_M = 3660$ K				
$H_F = 1.92 \times 10^5\ J/(kgK)$				
Coefficient	$C\ (J/kgK)$	$\eta\ (\Omega\text{-}m)$	$\kappa\ (W/mK)$	$\rho\ (kg/m^3)$
$a_S\ (-3)$	0	0	5.92816×10^{8}	0
$a_S\ (-2)$	0	0	-7.32997×10^{6}	0
$a_S\ (-1)$	0	0	4.57293×10^{4}	0
$a_S\ (0)$	1.11120×10^{2}	-9.68000×10^{-9}	7.93100×10^{1}	1.93000×10^{4}
$a_S\ (1)$	9.65140×10^{-2}	1.92740×10^{-10}	0	0
$a_S\ (2)$	-1.15270×10^{-4}	7.82600×10^{-14}	0	0
$a_S\ (3)$	7.63920×10^{-8}	-1.85170×10^{-17}	0	0
$a_S\ (4)$	-2.29720×10^{-11}	2.07900×10^{-21}	0	0
$a_S\ (5)$	2.70770×10^{-15}	0	0	0
$a_L\ (0)$	3.21750×10^{2}	1.31000×10^{-6}	7.05000×10^{1}	1.93000×10^{4}

The specific heat data of Ditmars, Cezairliyan, Ishihara, and Douglas[3] were used for molybdenum. The specific heat was held constant in the melting region, although data are available for molybdenum (and tantalum) to temperatures as high as 6900 K[4]. The specific heat of tantalum

[3] Ditmars, D.A., A. Cezairliyan, S. Ishihara, and T.B. Douglas, *Enthalpy and Heat Capacity Standard Reference Material: Molybdenum SR 781 From 273 to 2800 K*, (NBS SP-260-55). National Bureau of Standards, Gaithersburg, MD, September 1977.

[4] Shaner, J.W, G.R. Gathers, and C. Minichino, "Thermophysical Properties of Liquid Tantalum and Molybdenum," *High Temperatures-High Pressures*, Vol. 9, pp. 331-343, 1977.

was taken from the compilation in Touloukian and Ho[5]. Specifically, we used a second order polynomial fit to the data from References 3, 6, 7 and 12 of this compilation. The data of White and Collocott were used for the specific heat of tungsten to a temperature of 3400 K. Above that temperature, we used assumed values as described in Section 4.1.3 of this report.

As discussed earlier, thermal conductivity is not important in these experiments because of the short duration of the heating cycle, but the effect was included in the calculations. The data for molybdenum and tantalum were taken from Touloukian and Ho[6], whereas the tungsten data came from White and Collocott. For all three elements, the thermal conductivity in the melting region was held constant at the value associated with the melting temperature.

[5] Touloukian, Y.S., and C.Y. Ho, *Thermophysical Properties of Matter*, Vol. 4, Thermophysical Properties Research Center, Purdue University, Lafayette, IN, 1970.

[6] Touloukian, Y.S., and C.Y. Ho, *Thermophysical Properties of Matter*, Vol. 1, Thermophysical Properties Research Center, Purdue University, Lafayette, IN, 1970.

REPORT DOCUMENTATION PAGE

Form Approved OMB No. 0704-0188

1. AGENCY USE ONLY *(Leave blank)*	2. REPORT DATE	3. REPORT TYPE AND DATES COVERED
	November 2002	Final

4. TITLE AND SUBTITLE

Surface Heating of Molybdenum, Tantalum, and Tungsten Rods by Pulsed Currents

5. FUNDING NUMBERS

PR: 1L161102AH43

6. AUTHOR(S)

Hummer, C.R.; Powell, J.D.; Berning, P.R. (all of ARL)

7. PERFORMING ORGANIZATION NAME(S) AND ADDRESS(ES)

U.S. Army Research Laboratory
Weapons & Materials Research Directorate
Aberdeen Proving Ground, MD 21005-5066

8. PERFORMING ORGANIZATION REPORT NUMBER

9. SPONSORING/MONITORING AGENCY NAME(S) AND ADDRESS(ES)

10. SPONSORING/MONITORING AGENCY REPORT NUMBER

ARL-TR-2843

11. SUPPLEMENTARY NOTES

12a. DISTRIBUTION/AVAILABILITY STATEMENT

Approved for public release; distribution is unlimited.

12b. DISTRIBUTION CODE

13. ABSTRACT *(Maximum 200 words)*

Measurements of the surface voltage and surface temperature are made for small molybdenum, tantalum, and tungsten rods that have been subjected to pulsed electrical heating. The heating time is from 100 to 200 microseconds. The experimental results are then compared to results obtained from calculations undertaken with a numerical model that accounts for diffusion of current and ohmic heating within the sample. Good agreement between theory and experiment is obtained for the voltages and the temperatures. This agreement (a) provides valuable confirmation of the theoretical models and the experimental techniques used in Army applications of pulsed power; (b) demonstrates that the thermophysical properties of these substances are not affected by the rapid heating rates necessary in those applications; and (c) suggests a coupled experimental and theoretical technique for measuring resistivity in substances for which that property is not well known. The methodology for measuring the resistivity is developed and demonstrated in a sample experiment and calculation.

14. SUBJECT TERMS

electrical diagnostics
pulsed heating
thermophysical properties
voltage measurements

15. NUMBER OF PAGES

40

16. PRICE CODE

17. SECURITY CLASSIFICATION OF REPORT	18. SECURITY CLASSIFICATION OF THIS PAGE	19. SECURITY CLASSIFICATION OF ABSTRACT	20. LIMITATION OF ABSTRACT
Unclassified	Unclassified	Unclassified	